

**THREE-DIMENSIONAL RECONSTRUCTION
AND DESIGN OF PATIENT-SPECIFIC
IMPLANT USING OPEN-SOURCE SOFTWARE**

JOHARI BIN ABDULLAH

UNIVERSITI SAINS MALAYSIA

2019

**THREE-DIMENSIONAL RECONSTRUCTION
AND DESIGN OF PATIENT-SPECIFIC
IMPLANT USING OPEN-SOURCE SOFTWARE**

by

JOHARI BIN ABDULLAH

Thesis submitted in fulfilment of the requirements

for the degree of

Doctor of Philosophy

March 2019

ACKNOWLEDGEMENTS

I would like to acknowledge and thank my supervisors, Professor Dr. Zainul Ahmad Rajion, Professor Dr. Adam Husein, and Dr. Helmi Hadi for their help and support since I began my PhD. I have learnt so much from working with all of them and I have really enjoyed my time doing this study. Thanks particularly to Professor Dr. Zainul for helping me all the way from the start of this study and for encouraging me to overcome the obstacles along the way.

An enormous thank you goes to everyone attached with Biomaterials & 3D Visualization (Biom3d) Laboratory, especially to Abdul Manaf Abdullah, Suzana Yahya, and Associate Professor Dr. Dasmawati Mohamad; I learnt an incredible amount from all of you and loved working with you. Thanks to Neurosurgery team, Professor Dr. Zamzuri Idris and Dr. Low Peh Hueh for their assistance during hybrid cranial implant insertion into patients in the last stage. I would also like to thank Fairuz and Sham from the Dental Laboratory and Mohd Firdaus Daud and Fataha from the Radiology Department.

I would like to dedicate this work to my wife, Dr. Norsila Abdul Wahab who has inspired me to do a PhD, and my two children, Mikhael Johari and Misha Johari. I love all of you more than words can say.

I am grateful to Universiti Sains Malaysia for funding support for this research (RUT grant No. 1001/PPSG/852004 titled: Biomodelling for Cranio-Maxillofacial Reconstruction: Patient Specific, Aesthetic, Functional and Affordable Biomaterial Implants and Prostheses) and Ministry of Education for MyBrain15 scholarship.

TABLE OF CONTENTS

ACKNOWLEDGEMENTS	ii
TABLE OF CONTENTS	iii
LIST OF TABLES	vii
LIST OF FIGURES	viii
LIST OF ABBREVIATIONS	xix
ABSTRAK	xxi
ABSTRACT	xxiii

CHAPTER 1: INTRODUCTION

1.1 Background of the Study	1
1.2 Gap Statement and Justification of Study	3
1.3 Objectives of the Study	4
1.3.1 General Objective	4
1.3.2 Specific Objectives	4
1.4 Significance of the Study	5

CHAPTER 2: LITERATURE REVIEW

2.1 Craniofacial Region	7
2.2 Craniofacial Fractures	9
2.3 Imaging of Craniofacial Area.....	10
2.3.1 Conventional Radiograph	11
2.3.2 Computed Tomography Scan	12
2.4 Significance of the 3D Skull Models	13
2.5 Software for Skull Segmentation	15
2.5.1 Mimics v17.0 Software	16
2.5.2 MITK Workbench 2016.11 Software	17
2.5.3 3D Slicer 4.8.1 Software	19
2.5.4 InVesalius 3.1 Software	20
2.5.5 Summary of 3D Reconstruction Software	21
2.6 Design of Cranial Implant.....	23
2.6.1 Computer-Aided Design	23
2.6.2 Mirror Image Reconstruction Method	25
2.6.3 The Shape-Based Interpolation Method	26

2.7 Analyses of the 3D Skull Model and Cranial Implant	28
2.7.1 Craniometric Analyses	28
2.7.2 Geometric Analyses	30
2.8 Fabrication of Patient-Specific Cranial Implants in Patients with DC	32
2.9 Summary of Literature Review	33

CHAPTER 3: MATERIALS AND METHODS

3.1 Ethical Consideration	35
3.2 Study Design	35
3.3 Population and Sample.....	35
3.3.1 Reference Population	35
3.3.2 Sample Size Calculation	36
3.3.3 Patient Selection.....	36
3.3.4 Inclusion and Exclusion Criteria.....	36
3.4 Flowchart of the Study	37
3.5 Imaging Protocol	38
3.5.1 Image Acquisition	38
3.6 3D Reconstruction of the Skull	39
3.6.1 Mimics v17.0 Software	39
3.6.2 MITK Workbench 2016.11 Software	52
3.6.3 3D Slicer 4.8.1 Software	63
3.6.4 InVesalius 3.1 Software	71
3.6.5 Summary of Skull Reconstruction	76
3.7 Design of Cranial Implant.....	77
3.7.1 Designing Patient-Specific Cranial Implants using 3-Matic Software	78
3.7.3 Designing Cranial Implant using MITK Workbench 2016.11	91
3.7.4 Summary of Designing Cranial Implant	101
3.8 Analyses of the 3D Model and Cranial Implant.....	103
3.8.1 Craniometric Analyses	103
3.8.2 Geometric Analyses	109
3.9 Fabrication of Patient-Specific Cranial Implants using 3-Matic Software	111
3.9.1 Patient-Specific Hybrid Cranial Implants	112
3.9.2 Insertion of Cranial Implants in Patients with DC.....	114
3.10 Statistical Analyses	115

CHAPTER 4: RESULTS

4.1 Socio-Demographic Characteristics.....	116
4.2 Reliability and Accuracy Analyses	116
4.3 Craniometric Analyses	118
4.4 Geometric Analyses	120
4.4.1 3D Skull Models	120
4.4.2 Patient-Specific Cranial Implants	127
4.5 Cranial Implants in Patients with DC.....	129

CHAPTER 5: MEDICAL APPLICATIONS OF 3D MODELS

5.1 Pre-Operative Planning	132
5.2 Maxillofacial Prosthesis	135
5.3 Development of a New 3D Craniofacial Imaging Software in USM	140

CHAPTER 6: DISCUSSIONS

6.1 Software Used in this Study.....	143
6.1.1 Mimics v17.0 Software	143
6.1.2 MITK Workbench 2016.11 Software	145
6.1.3 3D Slicer 4.8.1 Software	146
6.1.4 InVesalius 3.1 Software	146
6.1.5 Usability of Software	147
6.2 The 3D Reconstruction of Skull.....	150
6.2.1 Accuracy Analyses.....	151
6.2.2 Reliability.....	153
6.3 Design of the Cranial Implant	155

CHAPTER 7: CONCLUSION AND FUTURE DIRECTION

7.1 Limitations of the Study.....	158
7.2 Recommendation for Future Research.....	159
7.3 Conclusion	159

REFERENCES.....	160
------------------------	------------

APPENDICES

APPENDIX A. ETHICAL APPROVAL

APPENDIX B. QUOTATIONS TO PURCHASE, RENT, AND RENEW LICENSE
FOR MIMICS SOFTWARE

APPENDIX C. LIST OF PUBLICATIONS

APPENDIX D. LIST OF MANUSCRIPTS

APPENDIX E. ACADEMIC ACTIVITIES

APPENDIX F. PERMISSION TO USE COPYRIGHTED MATERIALS

LIST OF TABLES

		Page
Table 2.1	Comparisons of a commercial software (Mimics) with three open-source software (MITK, 3D Slicer, InVesalius)	22
Table 3.1	Landmarks and their definitions for craniometric measurements	104
Table 3.2	List of the ten cranial measurements and their definitions used in this study	105
Table 4.1	Socio-demographic characteristics of subjects (n = 58)	116
Table 4.2	Intra-examiner reliability determined using ICC (n = 58)	117
Table 4.3	Intra-rater reliability for volume measurements for the first and second segmentation of the skulls using Mimics software (n = 58)	117
Table 4.4	One-way ANOVA for craniometric measurements of the four different software (n = 58)	119
Table 4.5	Dunnett test for craniometric measurements	120
Table 4.6	The 3D skull volume measurements using four different software	121
Table 4.7	Dunnett test for 3D skull volume	121
Table 4.8	Geometric analysis of the skull models using Hausdorff distance*	122
Table 4.9	Geometric analysis of the skull models using Dice similarity coefficient*	124
Table 4.10	The surface and volume of cranial implants designed using three different methods	127
Table 4.11	Geometric analysis of patient-specific cranial implants using Hausdorff distance*	128
Table 4.12	Geometric analysis of the patient-specific cranial implants using Dice similarity coefficient*	129
Table 4.13	The patients for hybrid cranial implants	130
Table 6.1	Number of steps needed for 3D reconstruction process	148

LIST OF FIGURES

		Page
Figure 2.1	Anterior view of the skull.	8
Figure 2.2	Lateral view of the skull.	8
Figure 2.3	Graphical user interface of Mimics software allows researcher to view images in axial, coronal, sagittal, and 3D views.	17
Figure 2.4	Graphical user interface of MITK software.	18
Figure 2.5	Graphical user interface of 3D Slicer software.	19
Figure 2.6	Graphical user interface of InVesalius software.	21
Figure 2.7	Graphical user interface of 3-matic software.	24
Figure 2.8	The mirror image reconstruction method using 3-matic software.	25
Figure 2.9	Shape-based interpolation of a prostate binary image derived from the manual segmentation of a CBCT image. 3D views of the original prostate (A), the same prostate with missing contours (B), and the interpolated prostate (C). [From Boydev <i>et al.</i> (2012), Figure 3, page 6, with permission].	27
Figure 2.10	The graphical user interface of CloudCompare software for geometric analyses of 3D skull model and patient-specific cranial implant.	30
Figure 2.11	DSC representing spatial overlap.	32
Figure 3.1	Flowchart of the study. The yellow circled numbers correspond to the objectives of this study.	37
Figure 3.2	The CT scan machine used in this study to acquire patients' CT images (CT Siemens Somatom Definition AS+ 128-slice).	38
Figure 3.3	The graphical user interface of introduction page after starting up Mimics software.	40
Figure 3.4	First, click "File" at the menu tools and select "New project wizard" to start the segmentation process.	40
Figure 3.5	Select folder files that contain DICOM data to import, then click "Next".	41
Figure 3.6	The software is reading the DICOM files in the chosen folder.	41

Figure 3.7	Click “Convert” to convert the DICOM files format into Mimics Project File.	42
Figure 3.8	The files were converting from DICOM format to Mimics Project File.	42
Figure 3.9	Click “OK” to confirm if the proposed orientation (anterior, posterior, left, right, axial, sagittal, coronal, bone, and soft tissue) was correct.	43
Figure 3.10	CT scan data in DICOM format that was finalised was successfully loaded in four views: (A) Coronal, (B) Axial, (C) Sagittal, and (D) 3D view.	43
Figure 3.11	Click “Segmentation” from the menu and select “Thresholding”.	44
Figure 3.12	At the “Predefined threshold sets” (red rectangle), choose for “Bone (CT)” where the HU was pre-set at 226 to segment the bone.	44
Figure 3.13	The “Green” mask was created (shown by the arrow) which constituted segmented bone. This can be seen as the green colour on the axial, coronal, and sagittal views.	45
Figure 3.14	Right click on the “Green” mask and select “Calculate 3D” to create the 3D skull model from the mask.	45
Figure 3.15	Choose “Optimal” to acquire the best quality of the 3D skull model and click “Calculate” to create the 3D skull model.	46
Figure 3.16	The 3D skull model obtained also included other objects (the three red circles) because they have similar HU value.	46
Figure 3.17	The 3D model obtained was processed using “Region Growing” method from the “Segmentation” menu list.	47
Figure 3.18	Click on any skull from any view. The region growing algorithm will connect all connecting pixels. Thus, other non-connected pixels (the red circles in Figure 3.16) will not be segmented anymore. “Yellow” mask was created.	47
Figure 3.19	Similar to earlier steps, right click on the “Yellow” mask which constituted segmented bone and select “Calculate 3D”.	48
Figure 3.20	The “Optimal” quality was chosen (arrow) and “Calculate” button was clicked (arrow) to create another 3D skull model from the “Yellow” mask.	48

Figure 3.21	The colour of the 3D skull model was changed to yellow but other objects were still in green, as shown in 3D view of the software. Next, untick the “Visibility” for green 3D objects to only show the isolated 3D model (yellow object) of the skull.	49
Figure 3.22	The final 3D skull model after post-processing steps. Only the yellow “3D Object” was visible in the 3D view of the software.	49
Figure 3.23	The “Export” on the menu list was clicked and the “Binary STL” was chosen (arrow) to export the 3D skull model to STL format.	50
Figure 3.24	To export the 3D skull model to STL format, first, click on the “Yellow” mask (1), then choose the output directory (2), then click “Add” (3). The output file name would appear on the software interface ‘Objects to convert’. Finally, click “Next” (4).	50
Figure 3.25	The “Optimal” button was chosen, and the “Finish” button was clicked. A final 3D skull model was saved in STL format.	51
Figure 3.26	The welcoming message in the graphical user interface after starting up MITK software.	52
Figure 3.27	First, click “Open File” at the menu tools; select the folder containing DICOM files, click one of the files, and click “Open” to start the segmentation process.	53
Figure 3.28	The “OK” button was clicked to load the files into MITK software.	53
Figure 3.29	CT data were successfully loaded in four views: (A) Axial, (B) Sagittal, (C) Coronal, and (D) 3D reconstruction view.	54
Figure 3.30	The “Window” from the menu list was clicked, the “Show View” was chosen and the “Segmentation” function was selected.	54
Figure 3.31	The 2D Tools (left) and 3D Tools (right) offered different type of segmentation methods in MITK software.	55
Figure 3.32	“Segmentation” tab was chosen, “Threshold” function was clicked, the value of 226 was inserted, then the “Confirm Segmentation” was clicked.	56
Figure 3.33	The “red” mask was created which constituted segmented bone. This can be seen as the red colour on the axial, coronal, and sagittal view.	56

Figure 3.34	The “Data Manager” tab was chosen, the segmented “skull” was right-clicked, and later the “Create smoothed polygon model” was clicked to create the 3D skull model.	57
Figure 3.35	By default in MITK software, the 3D skull model was created with 50% opacity as seen in the 3D view.	57
Figure 3.36	Right click on the “skull_smoothed” data, then drag the “Opacity” slider to the most right to disable the transparency (to have full opacity).	58
Figure 3.37	The 3D skull model was segmented together with other 3D objects as seen in the white circles.	58
Figure 3.38	The “Segmentation” tab was chosen and the “Picking” function was selected to isolate the skull from the other 3D objects.	59
Figure 3.39	The Shift keyboard button and mouse left click was pressed simultaneously while pointing on any part of the skull region to isolate the region of interest, then the “Confirm picked region” was clicked.	59
Figure 3.40	The “skull_picked” under the Data Manager menu was right-clicked and the “Create smoothed polygon model” was clicked to create the 3D skull model.	60
Figure 3.41	The new 3D skull model was constructed without noises. The “skull_smoothed” button was unticked to make the previous 3D skull model invisible.	60
Figure 3.42	The “skull_picked_smoothed” was right-clicked, then the “Opacity” slider was dragged to the most right to disable the transparency (to have full opacity).	61
Figure 3.43	The final 3D skull model was reconstructed using MITK software.	61
Figure 3.44	The “skull_picked_smooth” was clicked and the “Save” menu was clicked.	62
Figure 3.45	Folder was selected to save the file and the STL format was chosen.	62
Figure 3.46	The welcoming message in graphical user interface after starting up 3D Slicer software. The “Load DICOM Data” button was clicked to load data.	63
Figure 3.47	The “Import” menu was clicked, the DICOM folder was chosen and the “Import” button was clicked to import the DICOM files from the folder to 3D Slicer software.	64

Figure 3.48	The patient's data were selected and the "Load" button was clicked to load the data.	64
Figure 3.49	CT data were successfully loaded in four views: (A) Axial (B) 3D reconstruction view, (C) Sagittal, and (D) Coronal.	65
Figure 3.50	"Modules" menu was clicked, the "Segmentation" menu was chosen and the "Segment Editor" was clicked to start the segmentation process.	65
Figure 3.51	The "Add" button was clicked to create the segmentation (2) and the "Threshold" function was clicked.	66
Figure 3.52	The value of 226 was inserted in the "Threshold Range" and the "Apply" button was clicked to segment the skull from the soft tissues.	66
Figure 3.53	The "Show 3D" button was clicked to create the 3D skull model.	67
Figure 3.54	The skull was segmented together with other unwanted 3D objects as seen in the red circles in the 3D view of the software.	67
Figure 3.55	Under the same "Segment Editor" module, the "Islands" button was clicked, 'Keep largest island' was selected and "Apply" button was clicked.	68
Figure 3.56	The final 3D skull model after post-processing stage.	68
Figure 3.57	"Modules" menu was clicked, and the "Segmentation" menu was chosen.	69
Figure 3.58	The "Export" and "Models" buttons were selected, then the "Export" button was clicked to export the 3D skull model to STL format.	69
Figure 3.59	The "File" from the menu list was clicked and "Save" was chosen.	70
Figure 3.60	Other boxes in the "File Name" were unticked except for 'Segment_1.vtk'. Finally, the 3D skull model was saved in STL format.	70
Figure 3.61	Click "File" at the menu list and click "Import DICOM".	71
Figure 3.62	Select folder with patient's data and click "OK".	72
Figure 3.63	Click "Import" to load CT data into the InVesalius software.	72

Figure 3.64	The pre-defined threshold for bone was automatically set at 226. Click “Create Surface” to create 3D skull model.	73
Figure 3.65	The skull was segmented together with other unwanted 3D objects as seen in the red circles.	73
Figure 3.66	Click “Select largest surface” and click “Next step”.	74
Figure 3.67	3D skull model was created (Surface 2) without noises.	74
Figure 3.68	Click “Export data” menu and click “Export 3D surface”.	75
Figure 3.69	Save file in STL format and click “Save”.	75
Figure 3.70	Finally, the 3D skull models produced using different software: (A) Mimics, (B) MITK, (C) InVesalius, and (D) 3D Slicer are shown.	76
Figure 3.71	Summary of steps involved in 3D reconstruction of skull model for all four software. (A) DICOM format from CT scan data in sagittal view undergone segmentation to form (B) 3D skull model. (C) Post-processing image was formed after removing the noises. This image was then exported to (D) STL format for accuracy analyses.	77
Figure 3.72	The graphical user interface of 3-matic software.	78
Figure 3.73	The “File” menu was clicked and “Import Part” (arrow) was selected to import the STL format of skull with defect.	79
Figure 3.74	The patient’s file in STL format was chosen and the “Open” button was clicked to import the file.	79
Figure 3.75	The skull with cranial defect was loaded in 3-matic software.	80
Figure 3.76	The “Fix” menu was clicked and the “Reduce” function (arrow) was chosen to clean up the STL files.	80
Figure 3.77	The “Fix” menu was clicked and “Smooth” function (arrow) was chosen to smoothen the STL files.	81
Figure 3.78	The “Design” menu was clicked and “Wrap” function (arrow) was chosen to design the outline of the cranial implant.	81
Figure 3.79	The “View” menu was clicked, and the “Default Views” was chosen, followed by “Front” so that the skull faced anteriorly.	82
Figure 3.81	After creating a new sketch, under the sketch properties, the “Cells count” was changed from 10 to 100 to enlarge the sketch.	83

Figure 3.82	The sketch was enlarged once the “Cells count” was increased from 10 to 100 as seen in the red rectangle.	83
Figure 3.83	The “Align” menu was clicked and the “Interactive Translate” (arrow) and “Interactive Rotate” functions were used to adjust the sketch to be in the middle plane of the skull.	84
Figure 3.84	The sketch was adjusted (translate and rotate) to be located in the middle plane of the skull.	84
Figure 3.85	The sketch was located nicely in the middle plane of the skull and was ready for the mirror image function.	85
Figure 3.86	The “Align” menu was clicked and the “Mirror” function was selected to mirror the healthy part of the skull to the defected part.	85
Figure 3.87	The healthy part was mirrored to the defected part of the skull.	86
Figure 3.88	The “Align” menu was clicked and the “Interactive Translate” (arrow) and “Interactive Rotate” functions were used to adjust the position of the mirrored skull.	86
Figure 3.89	The “Design” menu was clicked and the “Boolean Subtraction” was chosen to subtract the healthy bone from the defected skull.	87
Figure 3.90	The “Finish” menu was clicked, and the “Trim” function was chosen to trim unwanted parts of the skull from the newly created implant.	87
Figure 3.91	The “Trim” function was used to cut out the unwanted parts by choosing “Remove inner” for trimming method.	88
Figure 3.92	The initial trim of the skull. The process was repeated until only the needed cranial implant was left.	88
Figure 3.93	Once the cranial implant was created, the “Finish” menu was clicked and the “Local Smoothing” function was chosen.	89
Figure 3.94	The cranial implant was tested for fitting at the defected skull.	89
Figure 3.95	The “File” menu was clicked, and the “Export” was chosen and the “STL” format was selected to save the cranial implant in STL format.	90
Figure 3.96	The patient-specific cranial implant was saved in STL format.	91
Figure 3.97	Fitting evaluation of patient-specific cranial implant on the defected skull.	91

Figure 3.98	The “Open” menu was clicked (1), one of the DICOM data were chosen (2), and the “Open” box was clicked (3).	92
Figure 3.99	The DICOM data were loaded in MITK. In the Data Manager tab, the working data were displayed (A). The axial slice was dragged to the left and right to view every slice of the image (B) in the ‘Image Navigator’ tab. The right red rectangle display (C) axial, (D) sagittal, (E) coronal, and (F) 3D views of the data.	92
Figure 3.100	The box next to the “Segmentation” menu was clicked to create a new segmentation (1) and the segmentation name was inserted (2).	93
Figure 3.102	The “Paint” tool was used to draw a line along defective skull.	94
Figure 3.103	The axial slice of the segmentation was enlarged to view the line drawn and for editing purposes.	95
Figure 3.104	Slices (A) 151, (B) 161, and (C) 171 of every tenth slice.	96
Figure 3.105	The “Interpolation” menu was enabled (arrow) to start the 2D shape-based interpolation.	96
Figure 3.106	The 2D shape-based interpolation was confirmed on all slices (1) and “Axial” slice menu was selected to proceed with the interpolation.	97
Figure 3.107	The 14 segmented axial slices for every tenth slice before the interpolation process (left) and after interpolation process (right) in coronal view.	97
Figure 3.108	The “cranial implant_smoothed” was right-clicked to move the “Opacity” slider to the right for full opacity.	98
Figure 3.109	Due to under-interpolation, not all surfaces of the implant were reconstructed, as shown in the green circles.	98
Figure 3.110	The final cranial implant before editing (left) and after editing (right).	99
Figure 3.111	Lines drawn on every tenth axial slice (left) and every fifth slice (right) on the coronal slice of CT data.	99
Figure 3.112	The 27 segmented axial slices for every fifth slice before interpolation (left) and after interpolation process (right).	100
Figure 3.113	The patient-specific cranial implant with every tenth slice interpolation (left) and every fifth slice interpolation (right).	100

Figure 3.114	The “cranial implant_smoothed” was right-clicked (1) and the cranial implant was saved (2) in STL format for further analysis.	101
Figure 3.115	Patient-specific cranial implant created with MITK: (A) every tenth slice interpolation, (B) every fifth slice interpolation, and (C) patient-specific cranial implant created using the gold standard 3-matic software.	102
Figure 3.116	Landmarks for the linear craniometric measurements.	103
Figure 3.117	Linear measurements of the 3D skull model.	105
Figure 3.118	The 3D model segmented using Mimics software (left) and the imported STL format in 3-matic software (right).	107
Figure 3.119	The 3D model segmented using MITK software (left) and the imported STL format in 3-matic software (right).	107
Figure 3.120	The 3D model segmented using 3D Slicer software (left) and the imported STL format in 3-matic software (right).	108
Figure 3.121	The 3D model segmented using InVesalius (left) and the imported STL format in 3-matic (right).	109
Figure 3.122	HD for two superimposed 3D skull models computed using CloudCompare software.	110
Figure 3.123	HD for two superimposed patient-specific cranial implants computed using CloudCompare software.	110
Figure 3.124	The final implant design was saved in STL format (left) and sent to 3D printer for fabrication (middle). The printed 3D model is on the right.	112
Figure 3.125	Gypsum mould was created using the fabricated patient-specific cranial implant.	112
Figure 3.126	DC patient’s autologous bone flap which was surgically taken out from the skull due to resorption.	113
Figure 3.127	PMMA resin was poured into gypsum mould that contained patient’s autologous bone flap.	113
Figure 3.128	The moulds were compressed to each other to give the hybrid implant its shape.	114
Figure 3.129	The mould and plastic were separated from the hybrid PMMA-autologous bone cranial implant after hardening.	114

Figure 3.130	The hybrid PMMA-autologous bone implant was fixed to the skull defect with titanium screws.	115
Figure 3.131	The hybrid cranial implant fit perfectly.	115
Figure 4.1	Author overseeing the process of preparing the hybrid cranial implant in the operation theatre.	130
Figure 4.2	Patient before (left) and after hybrid cranioplasty procedure (right).	131
Figure 4.3	The hybrid cranial implant fit perfectly.	131
Figure 5.1	A male patient attended Hospital USM with a complaint of swelling on his forehead which has been growing for the past one year.	132
Figure 5.2	CT scan showed dark fluid had resorbed the frontal bone of the patient but has not reached the brain.	133
Figure 5.3	The 3D skull model segmented using MITK software (left) and the printed 3D skull model (right) using Objet30 Scholar 3D Printer.	134
Figure 5.4	The printed 3D skull model was also used as a reference during surgery by the surgeons.	134
Figure 5.5	A 62 years old woman presented with severely painful skin ulcer, which later penetrated the skin, invading the bone beneath.	135
Figure 5.6	The hole was manually filled to cover the defect (left) on every fifth slice as seen in axial view (right).	136
Figure 5.7	Virtual try-in of the maxillofacial prosthesis in MITK software.	136
Figure 5.8	The 3D facial model reconstructed using open-source MITK software which was exported to STL format and sent to 3D printer for fabrication.	137
Figure 5.9	Printed 3D facial model for testing with the printed maxillofacial prosthesis.	137
Figure 5.10	Virtual 3D model (left) and printed physical 3D model (right).	138
Figure 5.11	Conversion of maxillofacial template (left) into wax model and later wax try-in (right).	139

Figure 5.12	Insertion of final prosthesis. (a) Outer surface, (b) Inner surface, and (c) Insertion.	139
Figure 5.13	A) Axial view of CT scan data with cranial bone fracture, (B) Fractured bone boundary curves reconstruction done as shown in red curves, and (C) Reconstruction of fractured part into DICOM format in the final stage.	141
Figure 5.14	NURBS curves were applied on every slice of axial view of CT scan.	141
Figure 6.1	Method to bypass post-processing steps in Mimics software: Tick “Keep largest” tool during the “Thresholding” process.	149
Figure 6.2	The steps involved in 3D reconstruction of skull models using four different software to achieve objectives 1, 2, and 3.	150
Figure 6.3	Superimposition of two skull models reconstructed using two different software. HD values represent the differences between them and DSC values represent their similarities.	152
Figure 6.4	Superimposition of two cranial implants designed using two different software. HD values represent the differences between them and DSC values represent their similarities.	153
Figure 6.5	The steps involved in designing the patient-specific cranial implant using two different software to achieve objectives 4, 5, and 6.	156

LIST OF ABBREVIATIONS

2D	Two-dimensional
3D	Three-dimensional
AM	Additive manufacturing
ANOVA	Analysis of variance
CAD	Computer-aided design
CAD/CAM	Computer-aided design/computer-aided manufacturing
CBCT	Cone beam computed tomography
CT	Computed tomography
DC	Decompressive craniectomy
DICOM	Digital Imaging and Communication in Medicine
DSC	Dice similarity coefficient
HD	Hausdorff distance
HU	Hounsfield unit
ICC	Intra-class correlation coefficient
MIROS	Malaysian Institute of Road Safety Research
MITK	Medical Imaging Interaction Toolkit
MRI	Magnetic resonance imaging

MVA	Motor vehicle accident
NURBS	Non-uniform rational B-spline
PACS	Picture Archiving and Communication System
PMMA	Polymethylmethacrylate
STL	Standard tessellation language

REKONSTRUKSI TIGA DIMENSI DAN MEREKA BENTUK IMPLAN SPESIFIK PESAKIT MENGGUNAKAN PERISIAN SUMBER TERBUKA

ABSTRAK

Perisian komersial bagi pengimejan perubatan kebiasaannya mahal. Malahan, kajian berkaitan rekonstruksi tiga dimensi (3D) tengkorak dan mereka bentuk implant spesifik pesakit menggunakan perisian sumber terbuka yang percuma adalah terlalu sedikit. Kajian ini bertujuan membandingkan model tengkorak 3D dan implant spesifik pesakit yang direkonstruksi daripada imej tomografi berkomputer (CT) menggunakan perisian sumber terbuka dengan perisian komersial. Pada peringkat pertama kajian ini, perisian komersial Mimics v17.0 telah digunakan untuk mengrekonstruksi model tengkorak 3D dari 58 orang peserta yang menjalani imbasan CT di Hospital USM. Seterusnya, tiga perisian sumber terbuka, MITK Workbench 2016.11, 3D Slicer 4.8.1 dan InVesalius 3.1, telah digunakan untuk mengrekonstruksi model tengkorak 3D dari peserta yang sama. Model tengkorak 3D yang dihasilkan dari perisian komersial dan sumber terbuka kemudiannya dieksport dalam format *standard tessellation language* (STL) ke perisian 3-matic v9.0 dan *CloudCompare* untuk dianalisis. Perisian SPSS versi 24.0 digunakan bagi analisis statistik. ANOVA satu hala menunjukkan tiada perbezaan yang bererti bagi analisis kraniometri yang dijalankan ke atas model tengkorak 3D yang direkonstruksi menggunakan perisian komersial dan tiga perisian sumber terbuka, $p > .05$. Analisis *Hausdorff distance* (HD) menunjukkan purata jarak titik di antara Mimics dengan MITK adalah 0.25 mm. Manakala, bagi Mimics dengan 3D Slicer, dan Mimics dengan InVesalius, hampir tiada perbezaan di antara dua model tengkorak 3D yang bertindih, iaitu

purata jarak titik adalah 0.01 mm. Dengan menggunakan analisis *Dice similarity coefficient* (DSC), persamaan di antara Mimics dan MITK, Mimics dan 3D Slicer, dan Mimics dan InVesalius adalah masing-masing 94.1%, 98.8%, and 98.3%. Pada peringkat kedua kajian ini, implan spesifik pesakit telah direka bentuk menggunakan perisian komersial 3-matic v9.0 dan perisian sumber terbuka MITK Workbench 2016.11 untuk 10 orang pesakit *decompressive craniectomy*. Kaedah interpolasi berasaskan bentuk digunakan, di mana teknik segmentasi setiap hirisan kelima dan kesepuluh data CT dilakukan. Reka bentuk akhir implan spesifik pesakit dari kedua-dua perisian dieksport ke format STL ke perisian *CloudCompare* untuk dianalisis. Hasil ujian Kruskal-Wallis bagi luas permukaan dan isipadu implan spesifik pesakit yang direka bentuk menggunakan 3-matic dan dua teknik MITK menunjukkan tiada perbezaan yang bererti, $p > .05$. Hasil analisis HD bagi implan spesifik pesakit yang direka bentuk menggunakan 3-matic dan dua teknik MITK menunjukkan purata jarak titik untuk 3-matic dengan MITK pada setiap hirisan kesepuluh adalah 0.28 mm dan bagi 3-matic dengan MITK pada setiap hirisan kelima adalah 0.15 mm. Hasil analisis DSC bagi implan spesifik pesakit yang direka bentuk menggunakan 3-matic dan dua teknik MITK menunjukkan persamaan di antara 3-matic dan MITK pada setiap hirisan kesepuluh dan kelima adalah masing-masing 85.1% dan 89.7%. Sebagai kesimpulan, perisian sumber terbuka yang dikaji dalam kajian ini adalah setanding dengan perisian komersial untuk rekonstruksi 3D berasaskan imej CT dan juga mereka bentuk implan spesifik pesakit. Ini adalah kajian pertama dalam mereka bentuk implan spesifik pesakit dari imej CT menggunakan kaedah interpolasi berasaskan bentuk dengan perisian sumber terbuka yang percuma.

THREE-DIMENSIONAL RECONSTRUCTION AND DESIGN OF PATIENT-SPECIFIC IMPLANT USING OPEN-SOURCE SOFTWARE

ABSTRACT

The commercial medical imaging software is typically expensive. Moreover, studies on three-dimensional (3D) skull reconstruction and design of patient-specific implant using free open-source software are scanty. This study aimed to compare the 3D skull models and patient-specific implants reconstructed from computed tomography (CT) images using the open-source software with commercial software. In the first stage of the study, the commercial Mimics v17.0 software was used to reconstruct the 3D skull models from 58 subjects who underwent CT scan at Hospital USM. Next, three open-source software, MITK Workbench 2016.11, 3D Slicer 4.8.1, and InVesalius 3.1, were used to reconstruct the 3D skull models from the same subjects. The 3D skull models from the commercial and open-source software were exported in standard tessellation language (STL) format into 3-matic v9.0 and CloudCompare software for analyses. SPSS version 24.0 was used for statistical analyses. For the first stage of the study, one-way ANOVA demonstrated that no significant difference was found on the craniometric analyses performed on 3D skull models reconstructed using the commercial software and the three open-source software, $p > .05$. Hausdorff distance (HD) analysis demonstrated the average points distance of Mimics versus MITK was 0.25 mm. Meanwhile, for Mimics versus 3D Slicer and Mimics versus InVesalius, there were almost no differences between the two superimposed 3D skull models with average points distance of 0.01 mm. Based on Dice similarity coefficient (DSC) analysis, the similarity

between Mimics and MITK, Mimics and 3D Slicer, and Mimics and InVesalius were 94.1%, 98.8%, and 98.3%, respectively. In the second stage of the study, patient-specific implants were designed using the commercial 3-matic v9.0 software and open-source MITK Workbench 2016.11 software for ten decompressive craniectomy patients. The shape-based interpolation method was used, in which the technique of segmenting every fifth and tenth slices of CT data were performed. The final design of patient-specific implants from both software was exported to STL format into CloudCompare software for analyses. Results of Kruskal-Wallis test for the surface and volume of patient-specific implants designed using 3-matic and the two MITK techniques showed no significant difference, $p > .05$. Results of HD analysis for patient-specific implants designed using 3-matic software and the two different MITK techniques showed the average points distance for 3-matic versus MITK on every tenth slice was 0.28 mm and for 3-matic versus MITK on every fifth slice was 0.15 mm. Results of DSC analysis for patient-specific implants designed using 3-matic and the two different MITK techniques showed the similarity between 3-matic and MITK on every tenth and fifth slices were 85.1% and 89.7%, respectively. In conclusion, the open-source software investigated in this study are comparable with the commercial software for 3D reconstruction of CT images as well as designing the patient-specific implants. This is the first study on designing patient-specific implant based on CT images applying shape-based interpolation method using the free open-source software.

CHAPTER 1

INTRODUCTION

Craniofacial fractures are commonly caused by motor vehicle accidents (MVA) including motorcycle, automobile, bicycle, and pedestrian hit (Naveen Shankar *et al.*, 2012; Pohchi *et al.*, 2013). MVA cases are also increasing in Malaysia (MIROS, 2017) and it costs Malaysia RM 9.2 billion in 2016 (Gan, 2017). Utilisation of three-dimensional (3D) reconstruction of the skull is a method to design a patient-specific cranial implant to improve management of patients with craniofacial fractures. The data obtained from the diagnostic imaging tools which were reconstructed in 3D with better resolution aid in the diagnosis to improve patient management.

1.1 Background of the Study

Our society places high regard on physical and facial beauty; no matter how loving, intelligent, or courageous a person may become, most will look no further than the face. Patients with craniofacial fractures and deformity normally have facial distortion. Apart from that, they may also suffer from other disabilities such as speech and visual impairment, eating and breathing disorders, and even brain dysfunction. Therefore, the impact of craniofacial fractures often causes its victim to have a lower quality of life, which may lead to isolation and rejection.

Craniofacial region of the human body is made up of various bones integrated in a complex fashion. Fractures of the craniofacial region can occur due to many factors such as sports-related injuries, gunshot trauma, and MVA. Reportedly, MVA-related was the most common (Hoppe *et al.*, 2014; Naveen Shankar *et al.*, 2012; Rivera-Barrios *et al.*, 2015). Different diagnostic imaging tools are being used to diagnose

fractures of the craniofacial region such as x-rays, computed tomography (CT) scan, and magnetic resonance imaging (MRI). As explained earlier, the craniofacial region has a complex anatomical setting and disruption in the bony continuity of this region is detrimental to both aesthetics and functionality. Due to these factors, it is always challenging to diagnose fractures of the craniofacial region. Most of the time, clinical examination is insufficient and requires radiological imaging tools to diagnose these fractures. With the advance in computer technology, 3D reconstruction of the craniofacial region can be achieved with the aim to get better visualization of the fractures to aid in diagnosis and management of the patients.

Cranial vault reconstruction is surgically performed to cover the defected bone in the skull which may be caused by congenital defects, diseases, accidents, infections, or tumours (Saldarriaga *et al.*, 2011). It is a complicated and risky endeavour involving intricate procedures that demand the skills and experience of oral and maxillofacial surgeons as well as plastic and reconstructive surgeons. The reconstruction of cranial defects is one of the few areas of reconstructive surgery where precision in pre-operative planning is vastly important.

Previously, surgical procedure for managing large defect of the skull is complicated as it has to be done manually based on two-dimensional (2D) imaging, namely the shaping, modelling, and placement of the implant, which is made of bone grafts, bone cements, or titanium meshes. Using this conventional method resulted in long and complex operations with poor aesthetic results. The manual process is very labour-intensive and expensive (Salmi *et al.*, 2012). With the advance in the computer and additive manufacturing (AM) technology, an implant that exactly fits

the defect can be manufactured pre-operatively from the radiographic data obtained from CT scan.

Poukens *et al.* (2008) highlighted the difficulties in cranial implants reconstruction if the injuries cross the midline of the skull. Designing an implant that involves part of the orbit is more complicated (Senck *et al.*, 2013) due to the curvature of the orbital area and the need for mirroring of the other side. Studies have reported the advantages of using several different computer-aided design and computer-aided manufacturing (CAD/CAM) platforms (Drstvensek *et al.*, 2008), which resulted in the perfectly fit implant, less surgery time, and better aesthetic results (Mazzoli *et al.*, 2009).

Cranial reconstruction of a very large defect in a skull is a challenge, as it normally involves the use of sophisticated proprietary image processing and expensive CAD software. As an alternative, open-source software is developed by a non-profit community or research organisation. It is free to use, distribute, and modify. Among the advantages of open-source software are its flexibility to modify features to fit the needs of the research and the ability to run experiments at a lower cost.

1.2 Gap Statement and Justification of Study

Following an extensive injury, surgical reconstruction can be very challenging due to limited 3D visualization. Visualizing these fractures in a form of a skull model would help in pre-operative planning of the case. In developed countries, 3D reconstruction was extensively applied in clinical setting unlike in Malaysia, where there is not many computer experts in 3D reconstruction to produce printed 3D models and patient-specific implants.

There are limited studies in comparing several open-source software with the commercial software in Malaysia. Therefore, the aim and scope of this study was to investigate, apply, and expand the application of several open-source software for 3D reconstruction of skull model and the design of patient-specific cranial implant.

1.3 Objectives of the Study

1.3.1 General Objective

The general objective of this study was to investigate and develop methods in using open-source software for 3D reconstruction and design of patient-specific cranial implant based on CT imaging and computer technology, and later to apply this method in clinical applications. Three different open-source software was compared with the commercial software on its accuracy in producing the 3D skull models. Later, the commercial and open-source software were utilised to design patient-specific cranial implants to be used in clinical cases.

1.3.2 Specific Objectives

The specific objectives for this study were:

1. To reconstruct 3D skull models using commercial software (Mimics v17.0) as the gold standard.
2. To investigate and develop methods to reconstruct 3D skull models using three open-source software:
 - a. MITK Workbench 2016.11 (German Cancer Research Center, <http://www.mitk.org>)
 - b. 3D Slicer 4.8.1 (National Institutes of Health, United States of America, <http://www.slicer.org>)

- c. InVesalius 3.1 (Centre for Information Technology, Ministry of Science and Technology, Brazil, <https://www.cti.gov.br/invesalius>)
3. To compare the craniometric and geometric measurements of 3D skull models reconstructed using Mimics software with MITK, 3D Slicer, and InVesalius software.
4. To design and fabricate patient-specific cranial implants using commercial software (3-matic v9.0) based on clinical cases from Neurosurgery Department, for insertion in patients with decompressive craniectomy (DC).
5. To design patient-specific cranial implants using open-source software (MITK) based on clinical cases from Neurosurgery Department.
6. To compare geometric measurements of patient-specific cranial implants produced using commercial software (3-matic) with open-source software (MITK).

1.4 Significance of the Study

As part of Universiti Sains Malaysia (USM) Research University Team (RUT) project, the author had investigated and applied several open-source software to perform image processing of CT data, to segment the region of interest of anatomical structures, to create 3D skull models, and finally to convert the 3D skull models to a format that is compatible for 3D printing platform.

Commercial software is expensive and not many hospitals or institutions have the budget to purchase them. Meanwhile, in-house software needs to be developed by the institution itself, which means they may need to hire an expert for this purpose. Thus, the use of open-source software to construct the 3D skull models and design of patient-specific cranial implants will reduce the cost of purchasing commercial

software as well as paying yearly licensing fee to maintain the software. Furthermore, it can benefit patients as their treatment time and cost would be much lower, apart from the more aesthetic results.

Research comparing open-source software with commercial software in their ability to reconstruct 3D skull models and design of patient-specific cranial implants is scanty. This study aimed to investigate this aspect to strengthen the concept that similarly accurate 3D skull models and good quality patient-specific cranial implants can be constructed using open-source software. Moreover, similar study to the present study can be replicated by other researchers from other health institutions or universities as the open-source software is freely available and the steps involved in using them were clearly outlined in this thesis.

Other ongoing research related to this topic which fall under the Craniofacial Imaging Research Cluster at USM involving inter-disciplinary team has produced significant benefits to the present patient management. Furthermore, there is an opportunity to enrich the training to other specialities using these data to demonstrate the importance of life-long learning. This study contributed to knowledge in medical imaging, open-source software technology, and clinical applications.

CHAPTER 2

LITERATURE REVIEW

The main goal of this chapter is to provide current concept of cranio- and maxillo-facial imaging of craniofacial fractures, the technology in 3D reconstruction of the skull based on CT scan data, and the design of cranial implant. The explanations include a review about the technology of imaging, the software for 3D reconstruction of the skull, and the software for implant design.

2.1 Craniofacial Region

Fractures of the craniofacial region can occur due to trauma, falls, and sports injury. A number of small bones join together to form the craniofacial region, adding to its complexity; thus, leading to difficulty in diagnosing and treating the fractures (Pickrell *et al.*, 2017; Shah *et al.*, 2016). The bones of the craniofacial region include bones around the eyes (orbital bones), cheekbones (zygoma), cranial bones (the top portion of the skull that protects the brain), frontal bone, lower jaw (mandible), nasal bones, upper jaw (maxilla), and parietal bones (Craven, 2014). Figures 2.1 and 2.2 show the anterior and lateral views of the skull, respectively.

Due to the complexity of this region (Patel *et al.*, 2016), having a good diagnostic tool to view these bones is helpful in clinical management. Different diagnostic imaging tools are being used to diagnose fractures of the craniofacial region such as x-rays, CT scans, cone beam computed tomography (CBCT) scans, and MRI. However, these images can only be viewed on a computer screen, which may limit a surgeon's perspective on the prognosis of repairing the fracture. Therefore, having a

3D model which can be derived from these data would greatly benefit surgeons in managing these fractures, especially when the fracture involved multiple small bones.

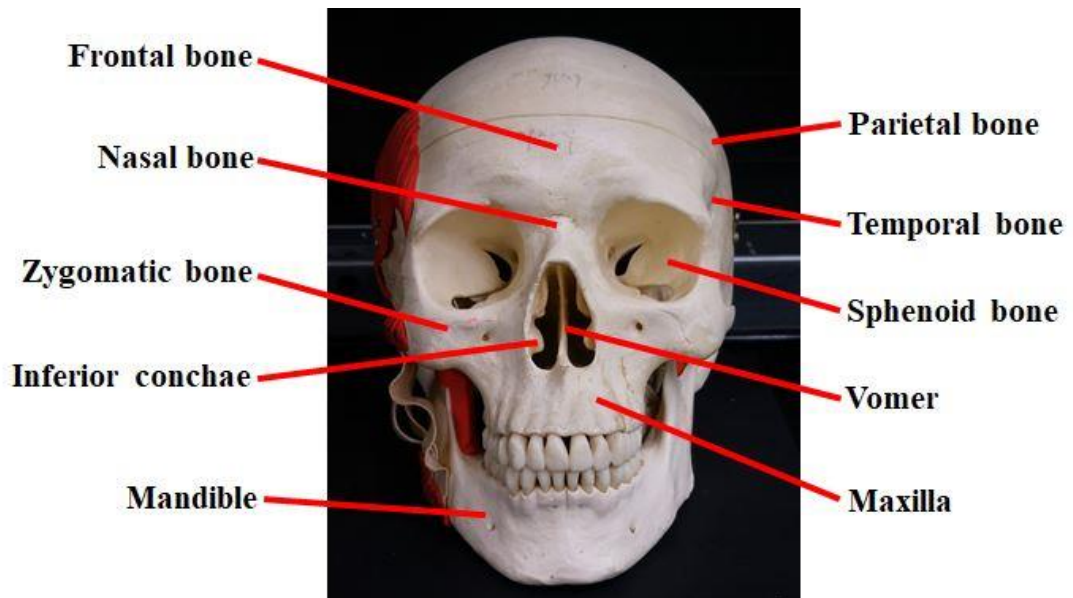


Figure 2.1 Anterior view of the skull.

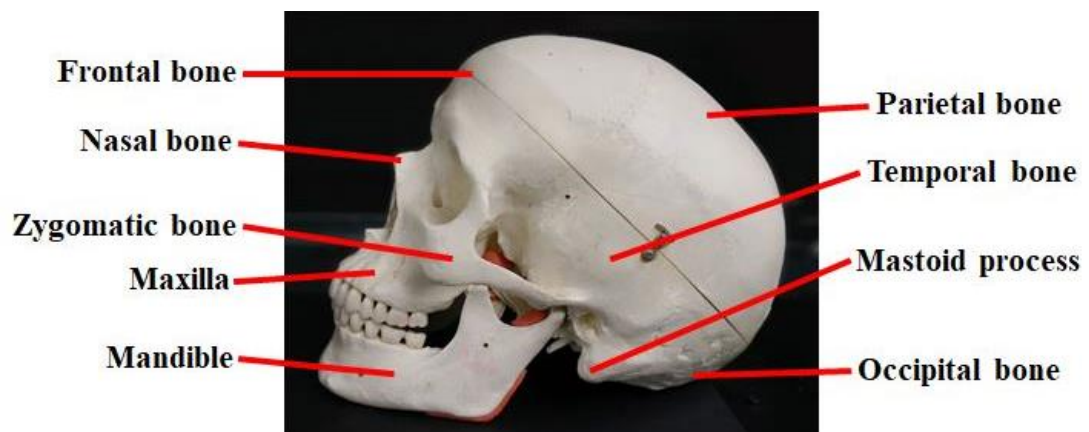


Figure 2.2 Lateral view of the skull.

3D anatomical models from medical imaging data provide the added benefit of allowing anatomist or anthropologist to avoid handling fragile “real” specimens. Often in forensic cases, there is residual soft tissue attached to the bony specimen that cannot be removed or defleshed. This soft tissue can obscure critical landmarks

and features used in establishing the biological profile or evidence of trauma. On the other hand, cadaveric dissection has always been associated with ethical concerns (Gunderman, 2008; Hasan, 2011), difficulties and potential risks of preservation, and disposal of specimens (Schmitt *et al.*, 2014). Furthermore, shortage of donors is another limitation associated with cadaveric dissection in some countries. With the 3D models, the soft tissue can be virtually removed or made transparent for analysis. Due to its precise reconstruction of intricate anatomical structures, there is an increasing use of 3D printing in medicine, ranging from basic anatomy to surgical practice and advanced research application (Chen *et al.*, 2017).

Detailed anatomical models replicated using 3D printers are best for teaching and learning of anatomy as they allow teachers and lecturers to introduce diverse specimens into classrooms (Thomas *et al.*, 2016). The printed 3D models are also useful to assist in diagnosis, surgical planning, implant design, and patient management (Giannopoulos *et al.*, 2016). Clinically, the 3D model is useful in management of craniofacial fractures.

2.2 Craniofacial Fractures

Common aetiological factors for craniofacial fractures include sports-related injuries, gunshot trauma, and MVA. Craniofacial fractures range from mild to severe. The primary goals in repairing complex craniofacial fractures are restoration of occlusion and mastication, and anatomic reconstruction of a symmetrical facial skeleton (Morrison *et al.*, 2014).

According to the report by Malaysian Institute of Road Safety Research (MIROS), 2012 Annual Report, the number of road accidents in Malaysia has increased year by

year, from 279,711 in 2002 to 462,423 in 2012. Furthermore, vehicle registration has also increased from 12 million in 2002 to 22.7 million in 2012. Although no specific study has been conducted on the relationship between the number of vehicles on the road and accident cases, common causes of craniofacial fractures were reportedly MVA-related, including motorcycle, automobile, bicycle, and pedestrian hit (Hoppe *et al.*, 2014; Naveen Shankar *et al.*, 2012; Rivera-Barrios *et al.*, 2015). Studies conducted by Pohchi *et al.* (2013) on maxillofacial fractures at Hospital Universiti Sains Malaysia (Hospital USM) also showed similar results.

Motorcycles crashes contributed to more than 60% of accidents in Malaysia, with overall fatality index of 22 /100,000 in the population in 2014, according to MIROS 2016 Annual Report (MIROS, 2017). Additionally, the report mentioned a statement from Malaysian Ministry of Transport in 2014 which stated that accidents involving commercial vehicles such as lorry, bus, and taxi are increasing, with the total of 57,430 road accidents in 2014 alone. All these accidents could potentially contribute to increased number of patients with craniofacial fractures.

Patients with craniofacial fractures often present with facial deformity and other physiological disorders such as impairment in speech, vision, eating, breathing, and brain dysfunction. For this reason, imaging of craniofacial fractures is very important to provide accurate and reliable information for a successful patient management.

2.3 Imaging of Craniofacial Area

Apart from clinical expertise, sophisticated radiological imaging is required to aid in the diagnosis of craniofacial fractures. Normally, craniofacial fractures are diagnosed from plain x-ray films, CT scan, and/or CBCT scan (Casselman *et al.*, 2013; Johari *et*

al., 2016; Li *et al.*, 2016). Commonly, CT scan is the chosen method for patients with craniofacial fractures (Bellamy *et al.*, 2013; Kennedy *et al.*, 2014; Munding *et al.*, 2016; Righi *et al.*, 2015) as it can show the bones clearly. The output of these CT scan's data is in the Digital Imaging and Communications in Medicine (DICOM) format, which is the international standard to transmit, store, retrieve, print, process, and display medical imaging information.

2.3.1 Conventional Radiograph

Imaging of anatomical structures for medicine began with the discovery of x-radiation by Wilhelm Roentgen in 1895 (Linnet *et al.*, 2012). For the first time, images of the internal body could be taken of living individuals. Marie Curie, who had just a few years before won a Nobel Prize for her research into radiation, drove a truck with portable x-ray equipment near the battlefields of France. This mobile unit allowed shattered bones to be visualized (Scatliff and Morris, 2014).

X-ray imaging involves taking a piece of film in a cassette and placing it between the object being imaged (body part) and the x-ray emission device or source. The film (or image capture receptor) detects the x-ray's waves and creates an image of the anatomy that it passed through. X-ray images are known to be effective at capturing bone and other dense structures but are less useful in distinguishing soft tissues. Although today's technology offers images of higher quality, more information can sometimes lead to diagnostic confusion (Scatliff and Morris, 2014). Not much information can be seen in a 2D modality; therefore, CT scan is more favourable for imaging of the craniofacial fractures because of its ability to visualise the fractures in 3D.

2.3.2 Computed Tomography Scan

CT scan was developed in the 1970s by Sir Godfrey Hounsfield and Allan MacLeod Cormack, and has become a critical diagnostic and imaging tool in both research and clinical settings (Wathen *et al.*, 2013). The technology works by acquiring planar x-ray images (or projections) taken at various degrees of rotation around a patient or specimen. These data are then reconstructed, typically with a filtered back projection algorithm, to produce a 3D array of radio-density values. The linear attenuation coefficient for each object at the selected effective energy was converted to Hounsfield Units (HU) using the standard equation (Reeves *et al.*, 2012):

$$\frac{\mu_x - \mu_{\text{water}}}{\mu_{\text{water}}} \times 1000 = \text{HU}$$

where μ is the linear attenuation coefficient and HU is the Hounsfield Unit. The Hounsfield number specifies the attenuation in relation to the attenuation in water. Each HU is equivalent to 0.1% of the attenuation of water, which represent the numerical value that is assigned to each pixel in a CT image.

The calibrated Hounsfield scale will have values of -1,000 HU to represent air, 0 HU to denote water, and up to 3,000 HU for dense bone. Soft tissues, which are primarily composed of water and protein, will have densities in the range of 100 to 300 HU (Bushberg *et al.*, 2012). However, it can be difficult to differentiate soft tissues via CT due to their low radio-opacity. On the other hand, the range for bone is either around 300 to 3000 HU (Schreiber *et al.*, 2011) or 150 to 2000 HU (Sogo *et al.*, 2012). The high range of bone HU is depending on the bone density. Hiasa *et al.* (2011) considered normal bone as having HU around 400 to 1000 HU.

The primary limitation of CT is its inability to distinguish many soft tissues based on native contrast. While bone has high contrast within a CT image due to its material density from calcium phosphate, soft tissue is less dense, and many are homogenous in density. This presents a challenge in distinguishing one type of soft tissue from another (Wathen *et al.*, 2013).

However, CT scans are good to project the bony contours of the anatomical location, and the 1-mm resolution is sufficient for diagnosis (Coolens *et al.*, 2009). The fractures site can be reconstructed to 3D images that makes it easier for both the radiologists and surgeons to diagnose and plan for treatment of the fractures.

2.4 Significance of the 3D Skull Models

Advances in craniofacial medical imaging have placed an importance of the 3D reconstruction of the skull model for medical applications. This technology has provided new possibilities to visualize complex medical data through generation of 3D skull models which were used for basic cranial education for medical students (Chen *et al.*, 2017), surgical training for surgeons (de Notaris *et al.*, 2014), pre-operative planning (Giannopoulos *et al.*, 2016), facial contouring surgery (Yim *et al.*, 2015), forensic medicine and dentistry (Katsumura *et al.*, 2016), computer-assisted surgery (Ritacco *et al.*, 2015), maxillofacial prosthesis (Jazayeri *et al.*, 2018), and craniofacial reconstruction (Jardini *et al.*, 2014; Maduri *et al.*, 2017; Park *et al.*, 2016; Schebesch *et al.*, 2013).

Craniofacial reconstruction is commonly performed following head or facial trauma and on cancer patients who have lost part of the bony structures following tumour surgery. In current practice, the reconstruction of craniofacial defects is normally

based on bone graft which is shaped to fit the defect. However, clinically, bone graft is limited to a small defect as the graft is taken from the patient's own bone. With 3D skull model derived from CT data, pre-surgical planning can be done to fabricate an implant from compatible biomaterials such as titanium mesh or methylmethacrylate (Jalbert *et al.*, 2014). Using this technique, bigger and complex defect of the skull can be repaired.

Sex determination from the unidentified human remains is now possible from the assessment of the 3D model of the skull. Results of studies by Dereli *et al.* (2018) on 85 3D skull models from archive of CT data and Shearer *et al.* (2012) on scanned 3D models of 128 dry skulls, showed that sex can be determined from morphological features in volume-rendered CT 3D images. Results from these studies, which rely only on the digital images without the need for maceration processes, and the transfer of digital data in place of physical material, will make it possible to gain expert opinions in forensic anthropology (Dereli *et al.*, 2018). This would hugely benefit the forensic community as the digital format would save cost and time.

Apart from forensic application, 3D model of the skulls could be used for teaching of difficult anatomical concepts (Pujol *et al.*, 2016) to medical and health sciences students (Chen *et al.*, 2017). With the 3D skull models, students will be able to place the models in their hands and have better understanding of the anatomical landmarks and their spatial relationship with other structures. Additionally, these 3D models are also helpful to illustrate anatomical variations among patients.

In summary, the 3D model of the skull can be used in pre-operative planning in maxillofacial-, neuro-, and plastic-surgery and its related disciplines, orthodontics, forensics medicine, anthropology, surgical simulation, face recognition, and many

other applications. In the medical imaging field, to find the most accurate, reliable, and yet low-cost 3D imaging software for 3D reconstruction of the skull is very important as it would have an impact on patient management. Therefore, it is important to find the best software for skull segmentation.

2.5 Software for Skull Segmentation

Most of the skull segmentation studies have utilised commercial software to create the meshed model or 3D model of the skull from patients' CT data; for example, Mimics software (Moiduddin *et al.*, 2017; Phanindra Bogu *et al.*, 2017; Rotaru *et al.*, 2012), CATIA software (Chrzan *et al.*, 2012), and Maxilim® software (Jonkergouw *et al.*, 2016). The 3D models created using skull segmentation software can be used for pre-operative planning or to design cranial implants (Kim *et al.*, 2012a). However, most of the software mentioned in the literatures are either commercial software or built in-house which were out of reach to researchers without big budgets or facilities.

Several studies have used open-source software, but no detailed steps were given as guidelines for other researchers to reproduce similar studies. Therefore, it was difficult to replicate these studies without proper tools or methods. Studies with detailed steps, particularly in the methodology of using certain open-source software would encourage other researchers to reproduce similar studies; therefore, encouraging more knowledge to be shared. Thus, this study was aimed to fill this gap.

Prior to the start of the study, apart from the commercial Mimics software available in Hospital USM, several open-source medical imaging software were downloaded

and tested. Three open-source software, Medical Imaging Interaction Toolkit (MITK), 3D Slicer, and InVesalius, were finally selected for the analysis based on their robustness, visualizations, reliability, and ease of use. Furthermore, these software were able to segment the 2D images and reconstructed them into 3D exportable models that is in STL files. An STL file describes the surface geometry of an object which can be sent to the 3D printers for printing of the skull.

2.5.1 Mimics v17.0 Software

Mimics software (Materialise NV, Heverlee, Belgium), has been widely used for reconstruction of 3D skull models and has been mentioned in many studies (Park *et al.*, 2016; Yuan *et al.*, 2017; Zhang *et al.*, 2018). Mimics is the shortened form for Materialise's Interactive Medical Image Control System, an interactive tool for the visualization and segmentation of CT images as well as MRI images and 3D rendering of objects.

This software is a fully-integrated, user-friendly 3D image processing and editing software based on various scanner data. It imports scanner data in a wide variety of formats and offers extended visualization and segmentation functions. The software is specially developed for image processing which converts the DICOM files into a 3D model. The obtained 3D model contains information about the patient's hard and soft tissues. Segmentation and region growing techniques were applied with different range of HU for the segregation of hard and soft tissues, making it suitable for the segmentation of the skull with craniofacial defect prior to craniofacial surgery (Moiduddin *et al.*, 2017). The software is also used for the 3D cephalometry analysis (Olmez *et al.*, 2011), reconstruction of 3D model of the skull (Bogu *et al.*, 2017; Decker *et al.*, 2013) and reconstruction of 3D model of the face (Decker *et al.*, 2013)

Most studies have used Mimics as a gold standard such as to evaluate the accuracy of image segmentation from the in-house computer-aided surgical simulation system for the orthognathic surgery (Yuan *et al.*, 2017). Similarly, Zale *et al.* (2018) studied the inter-departmental imaging protocol for 3D data of 30 CT scans by measuring glenoid version and they used Mimics software as the gold standard. The graphical user interface of Mimics software is shown in Figure 2.3.

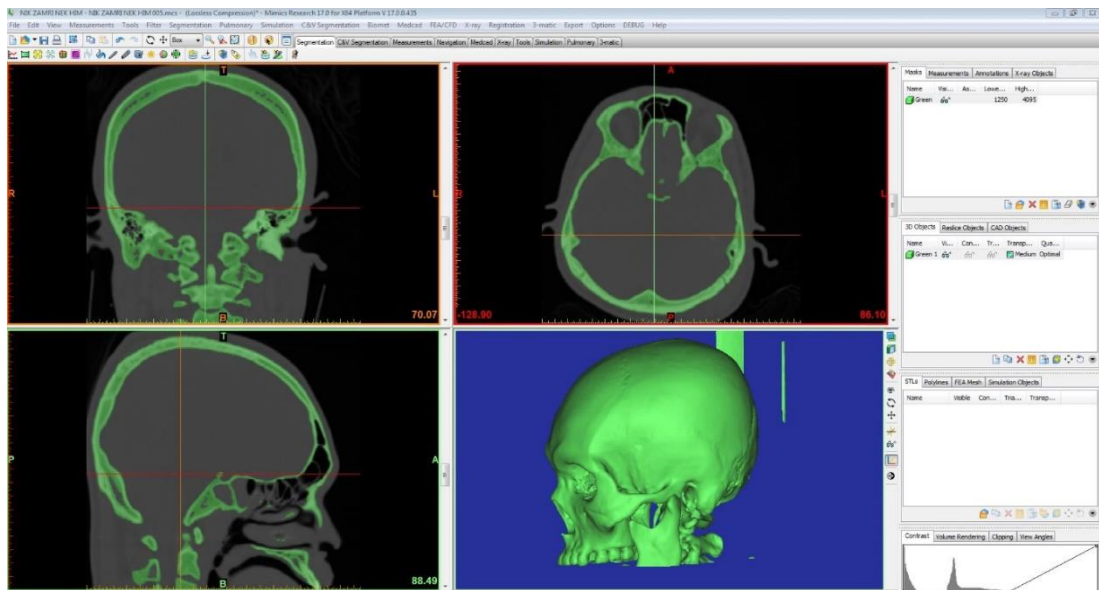


Figure 2.3 Graphical user interface of Mimics software allows researcher to view images in axial, coronal, sagittal, and 3D views.

Even though Mimics is a commercial software and the license has to be paid in order to use the software, the learning curve was quite steep to master the software interface and process. The training to use the software was also costly. Therefore, if this software can be replaced with one of the open-source software, the cost of hospital and patient management can be reduced.

2.5.2 MITK Workbench 2016.11 Software

MITK software was developed at the German Cancer Research Center (DKFZ) which can be downloaded at <http://www.mitk.org>. It is based on the well-established,

free open-source Medical Imaging Toolkit (MITK). It is available on multiple operating systems such as Microsoft Windows, GNU/Linux, and Apple Mac OS X. The software offers several interactive 2D and 3D segmentation tools for medical imaging data. Its framework allows interactive segmentation (Maleike *et al.*, 2009; Nolden *et al.*, 2013) with simultaneous image viewing and outlining of regions in axial, sagittal, and coronal orientations.

MITK has been used in several studies for 3D skull reconstruction for pre-operative planning (Martin *et al.*, 2014; Nolden *et al.*, 2013). In another study, MITK was used to segment proximal femur manually (as gold standard) and compared with a new method of graph cut segmentation (Pauchard *et al.*, 2016). Sporns *et al.* (2018) used MITK to compare segmentation results of swallowing muscles. The graphical user interface of MITK is shown in Figure 2.4.

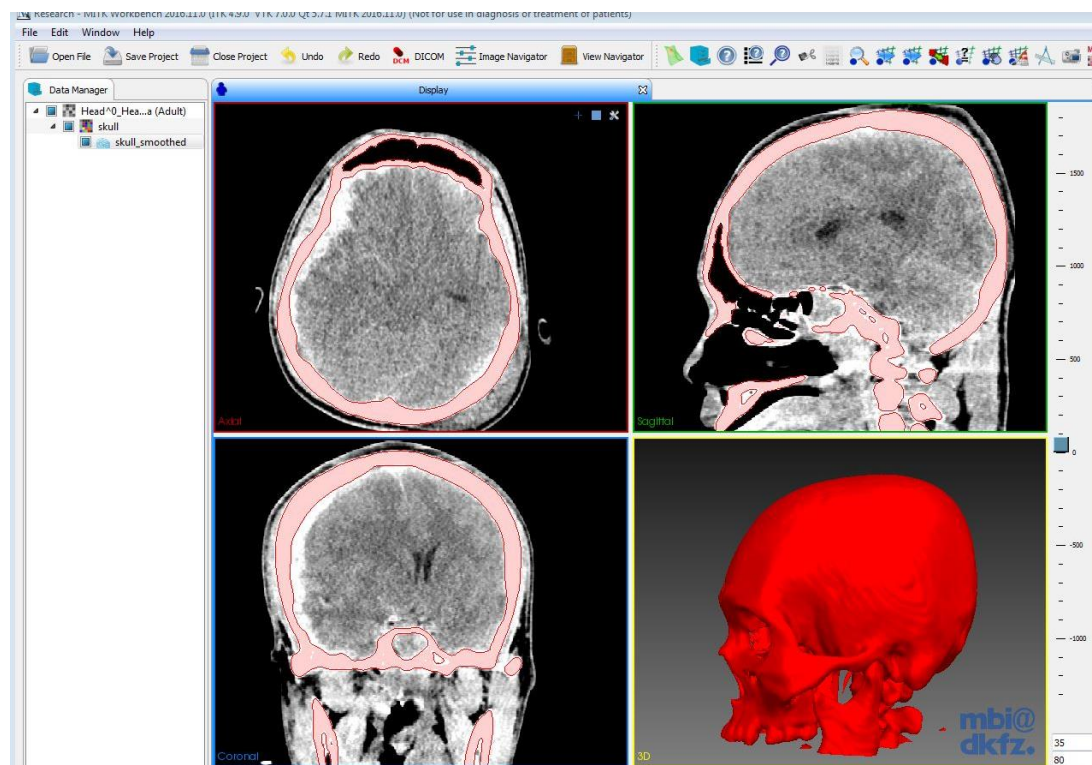


Figure 2.4 Graphical user interface of MITK software.

2.5.3 3D Slicer 4.8.1 Software

3D Slicer is another free open-source software which can be downloaded at <http://www.slicer.org>. It offers a platform for medical image informatics, image processing, and 3D visualization built through support from the National Institutes of Health, United States of America, and a worldwide developer community (Fedorov *et al.*, 2012). It is also available on multiple operating systems such as Microsoft Windows, GNU/Linux, and Apple Mac OS X with extensible plug-in for adding algorithms and applications. 3D Slicer has been used for volumetric analysis of medical images (Egger *et al.*, 2013) and reconstruction of 3D skull models (Szymor *et al.*, 2016; Tan *et al.*, 2016). The graphical user interface of 3D Slicer software is shown in Figure 2.5.

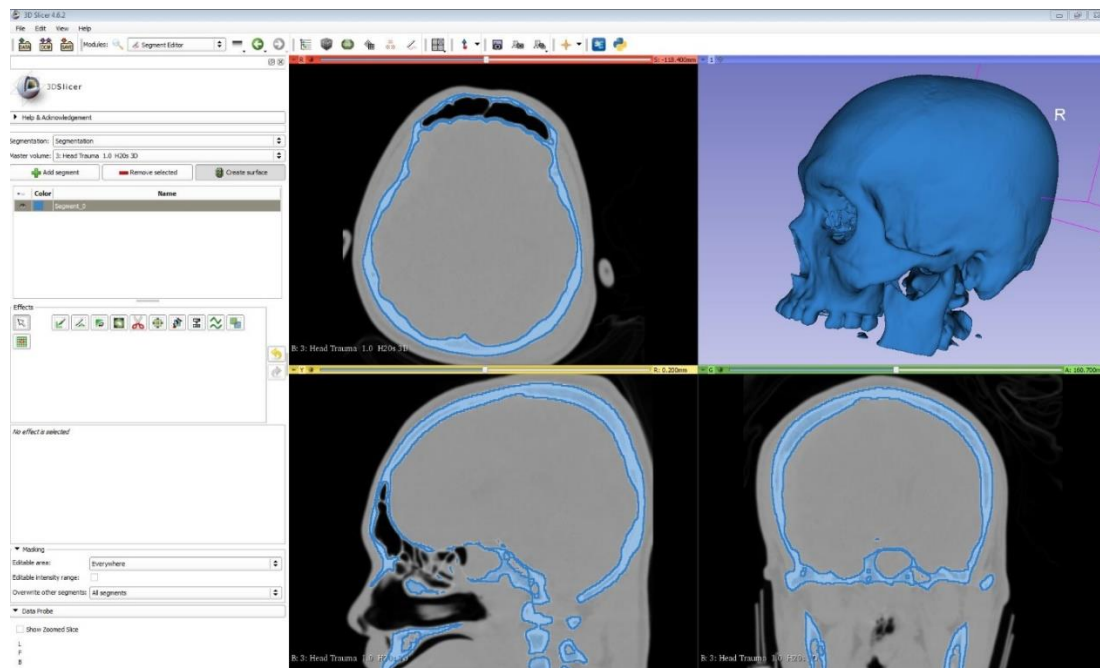


Figure 2.5 Graphical user interface of 3D Slicer software.

2.5.4 InVesalius 3.1 Software

InVesalius software is named in honour of the Belgian doctor Andreas Vesalius (1514-1564), widely considered as the father of modern anatomy. InVesalius software is developed in 2001 by the Centre for Information Technology (CTI), a unit of the Brazilian Ministry of Science and Technology. Initially, only the installation program was distributed as freeware. In November 2007 InVesalius software was made fully available as a free software and open-source via the Public Software Portal, allowing for communities of users and developers to connect. The software can be downloaded from the website <https://www.cti.gov.br/invesalius>.

InVesalius software is designed to run on personal computers such as desktop and notebooks, and it is compatible with various operating systems such as Microsoft Windows, GNU/Linux, and Apple Mac OS X. There are more than 10,000 people from 127 countries who are active users of InVesalius (Fazanaro *et al.*, 2016). This software has supported several surgeries in hospitals around the world for analysis and visualization of medical images. It has been used for the volumetric analysis of tumour (Gomes *et al.*, 2017), 3D reconstruction of skull model (Jardini *et al.*, 2016), and printing of anatomical structures (Coronel *et al.*, 2017).

InVesalius has been used for 3D reconstruction from CT data by many studies. Skrzat *et al.* (2016) reconstructed 3D skull models to enhance teaching of anatomy and claimed that the segmented 3D skull models were accurate; however, they did not do any comparison study to evaluate the accuracy. In another study, Ramos Verri *et al.* (2015) segmented six sets of mandible from CT data for biomechanical study of dental implant using InVesalius 3.0 and similarly, de Moraes *et al.* (2013) segmented three sets of mandible using InVesalius for finite element study of crown-

implant ratio on stress distribution. Another study was the segmentation of 3D craniosynostosis model of three patients and later sent to 3D printer for surgical simulation to simulate fronto-orbital advancement and posterior distraction in the operating room environment (Ghizoni *et al.*, 2018). Based on the capability of InVesalius in segmenting 3D models of bone as reported in many literatures, this software was chosen as one of the open-source software utilised in this study. The graphical user interface of InVesalius software is shown in Figure 2.6.

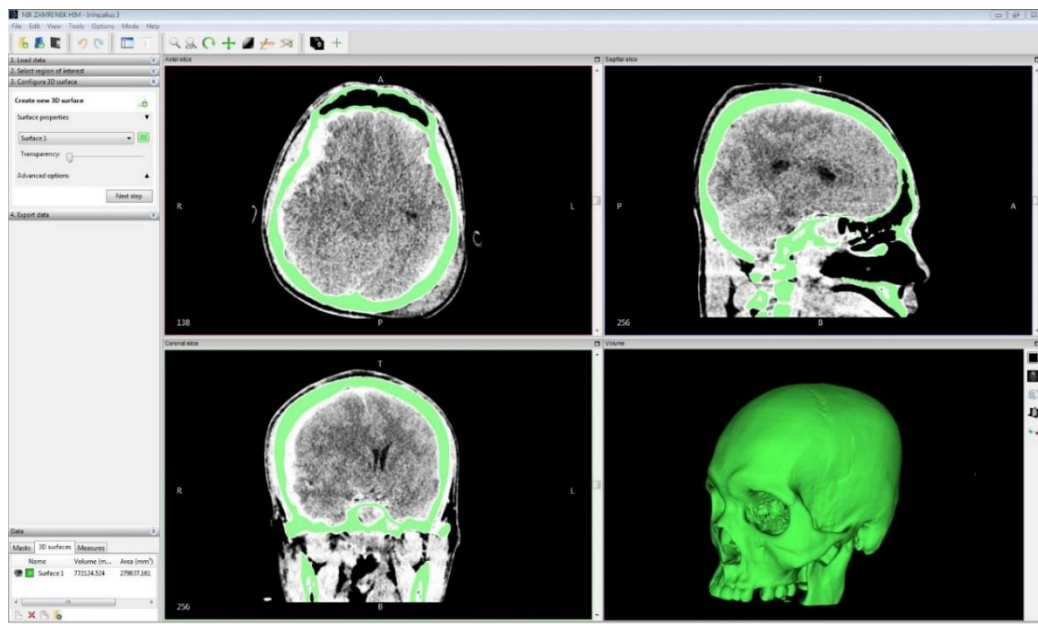


Figure 2.6 Graphical user interface of InVesalius software.

2.5.5 Summary of 3D Reconstruction Software

There were four software for skull segmentation reviewed in this chapter, which are the commercial Mimics software, and the three open-source software: MITK, 3D Slicer, and InVesalius. Table 2.1 compares these software in terms of their cost, country of origin, system requirements, input and output files format, and type of 3D models produced.

Table 2.1 Comparisons of a commercial software (Mimics) with three open-source software (MITK, 3D Slicer, InVesalius)

	Mimics v17.0	MITK Workbench 2016.11	3D Slicer 4.8.1	InVesalius 3.1
Cost	USD 58,500	Free	Free	Free
Country	Belgium	Germany	USA	Brazil
System requirements	Windows 7,8,10	Windows	Windows	Windows 7,8,10
		Linux	Linux	GNU/Linux
		Mac OS X	Mac OS X	Mac OS X
Input file	DICOM, BMP, JPEG, IGES, STL	DICOM, NRRD, VTK	DICOM, JPG, VTK, MRML, NRRD, OBJ, Analyze, NifTI	DICOM, Analyze
Output file	FEA Module e.g., Abaqus, ANSYS, COMSOL	VTK, VTP, PLY, STL	VTK, VTP, STL	OBJ, PLY, STL
	IGES, STL			
Type of 3D models	Surface-rendered	Surface-rendered	Surface-rendered	Surface-rendered
	Volume-rendered	Volume-rendered	Volume-rendered	Volume-rendered

2.6 Design of Cranial Implant

Functional and aesthetically-placed patient-specific cranial implants are extremely important for patients with large cranial defects. Therefore, pre-operative fabrication of the implants is recommended (Marreiros *et al.*, 2016) to ensure minimal adjustments during surgery, which would then translate to lower surgical cost and time, as the implants would fit nicely into the defect.

The techniques frequently used in designing cranial implants are CAD and mirror image reconstruction. However, the shape-based interpolation method may be another technique for this purpose, which was studied in this project.

2.6.1 Computer-Aided Design

Rapid developments in medical imaging and advances in CAD improved the quality of implants, resulted in improved aesthetic outcome as well as minimising operation time, blood loss, and risk of infection (Chen *et al.*, 2015; Zhao *et al.*, 2012). Patient-specific implants can be produced in any sizes with an accurate fit using this technology (Oh, 2018). The creation of the cranial implant with optimal size, shape, and mechanical properties prior to the surgical procedure reduces the operation time and complexity (Jardini *et al.*, 2014). The main advantage of using CAD is a better outcome and aesthetic of the implant; therefore, it can be successfully used in the repair of a defect (van der Meer *et al.*, 2013).

Using CAD software enables the users to automatically check if the design is within specification. It also enables users to view designs at an earlier stage in the design process. However, CAD software often consumes large amount of computer processing power. This requires a high-quality computer hardware that can be costly,

on top of the price of the CAD software (Nguyen *et al.*, 2018). The cost of hardware and software is a significant disadvantage of the CAD and a major barrier to adopt this technology, particularly for institutions with limited budget.

Another disadvantage of the CAD technology is the complexity of the software. As the CAD software advances, it becomes more flexible and adaptable and could do many things. However, this comes at the cost of making the software more complex. This complexity makes it more difficult for first-time users to master the software. Combined with the cost of training personnel in CAD technologies, this complexity represents another disadvantage of CAD.

One of the examples of CAD software is 3-matic software. It comes with standard sketcher and CAD functions and can work directly on STL levels or convert CAD data to STL. The graphical user interface of 3-matic software is shown in Figure 2.7.

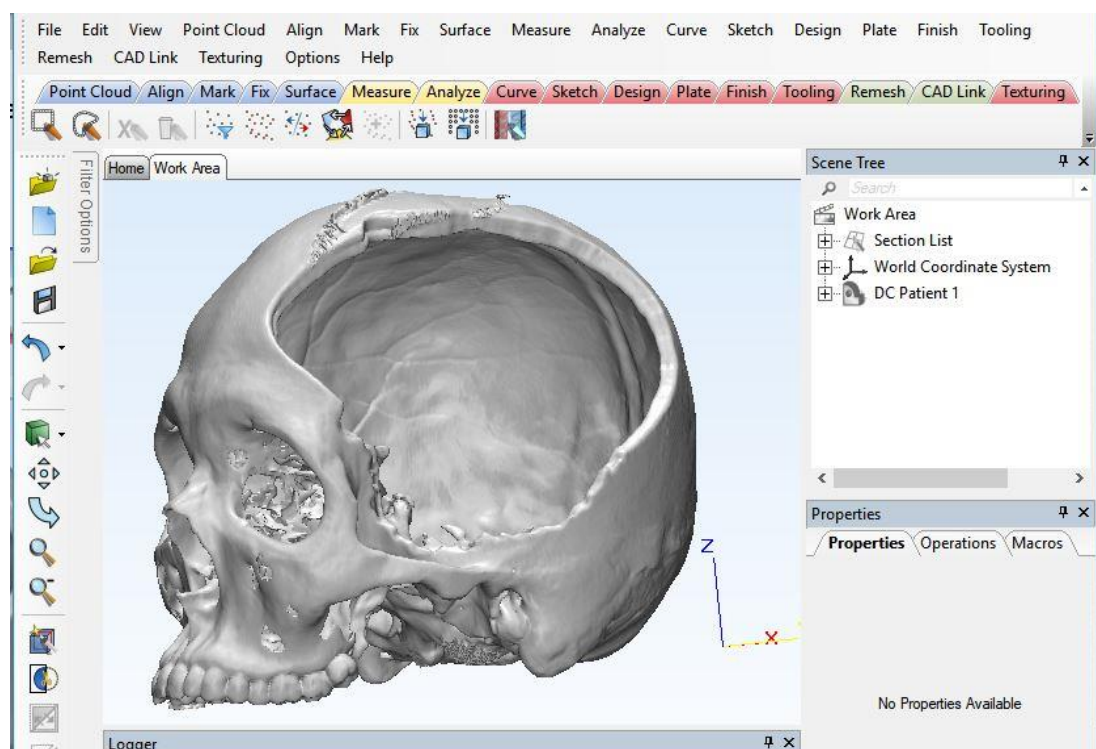


Figure 2.7 Graphical user interface of 3-matic software.